Absolute measurements of the high-frequency magnetic dynamics in high-T_c superconductors

ORNL/CP-95113

S.M. Hayden[a], G. Aeppli[b], P. Dai[c], H.A. Mook[c], T.G. Perring[d], S.-W. Cheong[e], Z. Fisk[f], F. Doğan[g], T.E. Mason[h]

CONF-970814--

[a] *H.H. Wills Physics Laboratory, University of Bristol, Bristol BS8 1TL, UK*

[b] *NEC Research Institute, Princeton, NJ 08540, USA*

[c] *Oak Ridge National Laboratory, Oak Ridge, TN 37831, USA*

[d] *Rutherford Appleton Laboratory, Chilton, Didcot, OX11 0QX, UK*

[e] *Bell Laboratories, Lucent Technologies, NJ 07974, USA*

[f] *Department of Physics, Florida State University, Tallahassee, Florida 32306, USA*

[g] *Department of Material Science and Engineering, University of Washington, Seattle, Washington 98195, USA*

[h] *Department of Physics, University of Toronto, Toronto, Canada M5S 1A7*

(7 August 1997)

Abstract

We review recent measurements of the high-frequency dynamic magnetic susceptibility in the high-T_c superconducting systems $La_{2-x}Sr_xCuO_4$ and $YBa_2Cu_3O_{6+x}$. Experiments were performed using the chopper spectrometers HET and MARI at the ISIS spallation source. We have placed our measurements on an absolute intensity scale, this allows systematic trends to be seen and comparisons with theory to be made. We find that the insulating $S = \frac{1}{2}$ antiferromagnetic parent compounds show a dramatic renormalization in the spin wave intensity. The effect of doping on the response is to cause broadenings in wave vector and large redistributions of spectral weight in frequency.

ORNL is managed by Lockheed Martin Energy Research Corp. under Contract No. DE-AC05-96OR22464 for the U.S. Department of Energy.

DISCLAIMER

I. INTRODUCTION

The collective excitations of the spins in the CuO_2 planes of the high temperature superconductors display a plethora of behavior [1], perhaps as exotic as the bulk properties themselves. A characterization of these excitations is motivated by several considerations. The spin excitations, which can be characterized by a well understood and easily interpretable probe such as neutron scattering, provide a window on the electronic correlations in these complex materials. Indeed Cooper pairing itself is a correlation between electron spins. A further motivation, especially in view of the unconventional pairing [2] in these materials, is that the magnetic excitations may be involved in the pairing attraction.

In the present paper we review our recent measurements [3–6] of the dynamic response over a wide frequency range i.e. up to energies of order $2J$. We find that in the superconductors there is significant spectral weight above the superconducting gap energy. Indeed, for both superconductors studied, the magnetic response $\chi''(q,\omega)$ is actually stronger for frequencies just above 2Δ than in the parent insulating antiferromagnet. We have been careful to convert our measurements into absolute units. This allows a systematic comparison between different systems, compositions and theories to be made.

II. EXPERIMENTAL

Our experiments were performed using the HET and MARI spectrometers at the ISIS pulsed spallation neutron source of the Rutherford Appleton Laboratory. HET and MARI are "direct geometry" chopper spectrometers. A pulse of neutrons of approximately 1 μs duration is produced when a 800 MeV pulsed proton beam hits a tantalum target. The neutrons are monochromated using a Fermi chopper at 10 m from the target appropriately phased to the proton pulse. Scattered neutrons are detected using 800 ^{3}He detectors 4 m from the sample.

Neutron scattering directly measures the imaginary part of the generalized magnetic

susceptibility $\chi''(\mathbf{Q},\omega)$. The scattering cross-section for an isotropic system is [7],

$$\frac{d^2\sigma}{d\Omega\, dE} = (\gamma r_e)^2 \frac{k_f}{k_i} |F(\mathbf{Q})|^2 \left(\frac{2\hbar V/\pi g^2 \mu_B^2}{1-\exp(-\hbar\omega/kT)} \right) \chi''(\mathbf{Q},\omega), \quad (1)$$

where $(\gamma r_e)^2$=0.2905 barn sr^{-1} μ_B^{-2}, $\mathbf{k}_i$ and $\mathbf{k}_f$ are the incident and final neutron wavevectors and $|F(\mathbf{Q})|^2$ is the magnetic form factor. Absolute unit conventions were performed by measuring the elastic incoherent scattering from a vanadium standard [8] under the same experimental conditions and by measuring the low-frequency coherent phonon scattering from the sample [9]. Throughout this paper, we label momentum transfers (Q_x, Q_y, Q_z) in units of Å^{-1} by their reciprocal space positions $\mathbf{Q}$=(h,k,l)= $(2\pi Q_x/a, 2\pi Q_y/b, \pi Q_z/c)$. Following previous practice, we use the *orthorhombic* nomenclature to label reciprocal space in the $La_{2-x}Sr_xCuO_4$ system and *tetragonal* nomenclature in the $YBa_2Cu_3O_{6+x}$ system. This means that the CuO_2 planes are parallel to (010) in $La_{2-x}Sr_xCuO_4$ and (001) in $YBa_2Cu_3O_{6+x}$. Details of the samples are given elsewhere [3–6]. In the case of the $La_{2-x}Sr_xCuO_4$ system data was collected with the (001) plane coincident with the principal scattering plane of the spectrometer. For $YBa_2Cu_3O_{6+x}$, the $(1\bar{1}0)$ plane was used.

III. THE QUANTUM ANTIFERROMAGNETS

We first discuss the parent antiferromagnets La_2CuO_4 and $YBa_2Cu_3O_{6.15}$. For the purpose of this paper, we model the systems as a set of weakly coupled CuO_2 layers or bilayers. In this case, the high-frequency spin excitations can be described by the Heisenberg Hamiltonian for a single CuO_2 layer or bilayer,

$$H = \sum_{ij} J_{\parallel}\, \mathbf{J}_i \cdot \mathbf{J}_j + \sum_{ij'} J_{\perp}\, \mathbf{J}_i \cdot \mathbf{J}_{j'}. \quad (2)$$

The first term in Eq. 2 represents the nearest-neighbor coupling between Cu spins in the same CuO_2 plane. The second term (not present in the single layer compound) represents the coupling between nearest-neighbor Cu spins in different layers.

In the case of the single layer compound ($J_\perp = 0$), conventional spin-wave theory in the classical large-S limit yields the dynamic susceptibility

$$\chi''(\mathbf{Q},\omega) = Z_\chi \, \pi \, g^2 \, \mu_B^2 \, S \left(\frac{1-\gamma(\mathbf{Q})}{1+\gamma(\mathbf{Q})}\right)^{1/2} \delta\left(\hbar\omega \pm \hbar\omega(\mathbf{Q})\right), \tag{3}$$

where,

$$\hbar\omega(\mathbf{Q}) = 2J_{\|}\left[1-\gamma^2(\mathbf{Q})\right], \tag{4}$$

and $\gamma(\mathbf{Q}) = \cos(\pi h)\cos(\pi l)$. We have included a "quantum renormalization" of the overall amplitude Z_χ. In the conventional linear spin-wave model applicable for large S, $Z_\chi = 1$. For small S, quantum corrections [10,11] become important (the Neel state is not a good approximation to the ground state) leading to a renormalization of the overall scale of the spin-wave dispersion and to a reduction in magnetic response with respect to the classical spin-wave theory. The renormalization of the overall scale can be included in the exchange constant $J^* = Z_c J$, where J is the exchange constant occurring in Eq. 2 and J^* that obtained from the measured dispersion interpreted using an equation such as Eq. 4. The value of Z_χ *can* be obtained by neutron scattering, if measurements are placed on an absolute intensity scale. However, Z_c *cannot* be measured directly from neutron scattering and must be estimated from theory. In the case of the $S = \frac{1}{2}$ square-lattice antiferromagnet, Singh [10] and Igarashi [11] have estimated $Z_c = 1.18$ and Z_χ=0.51 based on a $1/S$ expansion.

The presence of the second term (i.e. $J_\perp \neq 0$) in Eq. 2 leads to the existence of two branches in the spin-wave dispersion which can be labeled according to whether neighboring spins in different planes rotate in the same direction ("acoustic" or "odd" mode) or in opposite directions ("optical" or "even" mode) about their time-averaged directions. In the conventional linear spin-wave approximation, the acoustic and optic modes have the response functions [12]

$$\chi''_{\rm op}(\mathbf{Q},\omega) = Z_\chi \, \pi \, g^2 \, \mu_B^2 \, S \left(\frac{1-\gamma(\mathbf{Q})+J_\perp/J_{\|}}{1+\gamma(\mathbf{Q})}\right)^{1/2} \tag{5}$$

$$\times \sin^2\left(\frac{\pi \, \Delta z \, l}{c}\right) \delta\left(\hbar\omega \pm \hbar\omega_{\rm op}(\mathbf{Q})\right) \tag{6}$$

and

$$\chi''_{\rm op}(\mathbf{Q},\omega) = Z_\chi\,\pi\,g^2\,\mu_{\rm B}^2\,S\left(\frac{1-\gamma(\mathbf{Q})}{1+\gamma(\mathbf{Q})+J_\perp/J_{||}}\right)^{1/2} \tag{7}$$

$$\times\cos^2\left(\frac{\pi\,\Delta z\,l}{c}\right)\delta\left(\hbar\omega \pm \hbar\omega_{\rm ac}(\mathbf{Q})\right), \tag{8}$$

respectively. The dispersion relations are

$$\hbar\omega^{\rm ac}_{\rm op}(\mathbf{Q}) = 2J_{||}\left\{1-\gamma^2(\mathbf{Q})+J_\perp/J_{||}\left[1\pm\gamma(\mathbf{Q})\right]\right\}^{1/2}, \tag{9}$$

where $\gamma(\mathbf{Q}) = \frac{1}{2}[\cos(2\pi h)+\cos(2\pi k)]$ and Δz= 3.2 Å is the separation of the CuO_2 planes in a bilayer. The inter-planer coupling term in Eq. 2 leads to no additional dispersion along the z-direction, only a modulation in the amplitude of the response which nevertheless can be used to distinguish between the two modes.

A. La_2CuO_4

The two-dimensionality of the scattering in La_2CuO_4 means that we are able to cut through the spin waves at several energy transfers for a single spectrometer setting. Fig. 1 shows data collected for E_i =300 meV and $\mathbf{k}_i \parallel (010)$ on the MARI spectrometer. Panels (b)-(f) show constant energy cuts along the (1,0,0) direction. A spin-wave peak is observed near $h = 1$. Twin peaks due to spin waves propagating in opposite directions are not observed due to the poor out-of-plane resolution in the (001) direction. The broadening in the peak at higher frequencies is due to the spin-wave dispersion. A convenient way to display the data in Fig. 1 is as a local- or wavevector-integrated susceptibility $\chi''(\omega) = \int_{\rm BZ}\chi''(\mathbf{Q},\omega)\,d^3Q/\int d^3Q$, this is shown in Fig. 2(a). The solid lines in Fig. 1(b)-(f) and Fig. 2 are fits to the spin-wave model described by Eq. 3. Quantitative analysis yields an exchange constant consistent with our previous determination [3] J^* =153 meV and $Z_\chi = 0.39\pm0.1$. This is in agreement with the calculation of Igarashi [11] and demonstrates the importance of quantum corrections in this system.

B. $YBa_2Cu_3O_{6.15}$

As discussed above, the bilayer nature of this material results in two collective modes with additional structure to $\chi''(\mathbf{Q},\omega)$ as compared with the single layer material. The optic mode has a gap at the 2-D magnetic zone centers such as $(\frac{1}{2}\frac{1}{2}l)$ of $\hbar\omega_g = 2\sqrt{J_\perp J_{||}}$. Its intensity displays an overall modulation $\cos^2(\pi\,\Delta z\,l/c)$ which has maxima at positions $l = 1.8, 5.5, \ldots$. Correspondingly, the acoustic mode has an overall modulation of $\sin^2(\pi\,\Delta z\,l/c)$ and therefore has maxima at $l = 3.7, 7.3, \ldots$. We are able to probe the spin waves at various values of $\hbar\omega$ and l by varying the incident energy. Fig. 3(b)-(e) show data collected for different energy transfers at l values corresponding to positions where the scattering is predominately acoustic. As in La_2CuO_4, a peak is observed near the magnetic zone center, for all energy transfers investigated, due to propagating spin waves. Similar cuts probing l values, where the optic mode dominates, are shown in Fig. 3(g)-(j). In this case, no peak is observed at the lowest energies because these are below the optic gap. A more convenient way to look at this data is in the form of a local susceptibility (see above). Fig. 4 shows the contributions of the two branches to the local susceptibility extracted from the data in Fig. 3. When the data are plotted in this way, we see that the optic and acoustic contributions are equal at higher frequencies. While below $\hbar\omega_g$, the contribution from the optical mode is zero within the experimental error. A detailed analysis [5] yields a value for the optic gap of $\hbar\omega_g = 74 \pm 5$ meV. A similar value for the optic gap was obtained using reactor-based instrumentation [13].

In order to determine the exchange constant $J_\perp$ describing the coupling of spins in different planes, we also need to know $J_{||}$ because the optic gap is $\hbar\omega_g = 2\sqrt{J_\perp J_{||}}$. The in-plane exchange coupling, $J_{||}$ can be obtained from a measurement of the high-frequency spin waves. Fig. 5 shows data collected with the higher incident energy E_i =600 meV. We note that for energy transfers above 245 meV there is little variation in the intensity, suggesting that this energy is close to the zone boundary energy. A simultaneous resolution-corrected fit of the linear spin wave model (Eqs. (5)-(7)) to all our data yields values for the exchange

constants of $J_{\|}^{*} = 125 \pm 5$ meV and $J_{\perp}^{*} = 11 \pm 2$ meV. Further, since our measurements are in absolute units we are able to estimate the amplitude renormalization. We find a value of $Z_{\chi} = 0.4 \pm 0.1$, again the quantum renormalization is close to the value predicted by a $1/S$ expansion ($Z_{\chi} = 0.51$).

IV. THE SUPERCONDUCTORS

Of particular interest is the nature of the spin fluctuations [14,4] for metallic and superconducting compositions . We have therefore studied the compounds $La_{1.86}Sr_{0.14}CuO_4$ (a composition close to optimal doping) and $YBa_2Cu_3O_{6.6}$ (an underdoped superconductor). In both cases we find strong high-frequency spin fluctuations in the superconducting state.

A. $La_{1.86}Sr_{0.14}CuO_4$

Fig. 1(h)-(l) shows data collected for $La_{1.86}Sr_{0.14}CuO_4$ under the same conditions as Fig. 1 and in the *same units*. Doping has a dramatic effect on the magnetic excitations: at low frequencies, the peaks are broader in reciprocal space and at higher frequencies there is a large suppression of the intensity. At the highest frequencies, the peaks appear to be disappearing more rapidly in the superconductor than the insulator. This can be seen clearly when we extract and plot the local susceptibility in Fig. 2(b). When we include low frequency data from a reactor-based experiment, it becomes clear that the local response is peaked near 22 meV. Thus doping leads to a shift of spectral weight to intermediate energies.

B. $YBa_2Cu_3O_{6.6}$

The low frequency dynamics of superconducting $YBa_2Cu_3O_{6+x}$ have been the subject of considerable investigation [1]. The $YBa_2Cu_3O_{6.6}$(T_c = 62.7 K) sample used in the current study is of high quality: it shows a sharp "resonance peak" [15] at 34 meV on entering the superconducting state and has recently been shown [16] to develop incommensurate peaks in

$\chi''(\mathbf{q},\omega)$ for frequencies near 25 meV. We concentrate here on the nature of the dynamics for temperatures just above the superconducting transition temperature. Fig. 6 shows inelastic data collected for $T = 80$ K on the MARI spectrometer in a similar manner to that in Fig. 3. The reader should note that the energies chosen in Fig. 6 are different to Fig. 3 because of the different detector positions on the HET and MARI spectrometers. By assuming the scattering has a Gaussian wavevector dependence for each energy, we have extracted the frequency variation of the acoustic and optical contributions to the local susceptibility $\chi''(\omega)$ from data such as that shown in the figure. This is shown in Fig. 7.

Comparison of Figs. 6 and 7 with Figs. 3 and 4 shows that the magnetic response has changed dramatically between the metal and the insulator. This is well known at low frequencies [1], as in $La_{2-x}Sr_xCuO_4$ there is a large broadening of the low frequency peak in wavevector. More dramatic is the redistribution of spectral weight in energy revealed by the local susceptibility in Fig. 7. Inspection of Fig. 4 and Fig. 7, which are in *the same units* and therefore can be directly compared, shows that doping causes a shift of spectral weight from high frequencies (above 100 meV) into the range around 50-100 meV. The gap in the optic fluctuations remains and is possibly slightly reduced.

V. DISCUSSION

Our measurements of $\chi''(\omega)$ on La_2CuO_4 and $YBa_2Cu_3O_{6.15}$ are summarized in Fig. 2(a) and Fig. 4. We note that observed $\chi''(\omega)$ for La_2CuO_4 and the acoustic branch of $YBa_2Cu_3O_{6.15}$ are of approximately equal intensity: the units of the susceptibility are expressed per formula unit in both cases, $YBa_2Cu_3O_{6+x}$ has two Cu in the CuO_2 planes per formula unit. When we compare our measurements on the quantum antiferromagnets La_2CuO_4 and $YBa_2Cu_3O_{6.15}$ with linear spin-wave theory. We find that, in both cases, the dispersion and amplitude variation are well accounted for. However, an overall renormalization of the amplitude Z_χ must be included to account for the observed intensity of the one-magnon response. Our observations agree with calculations of Z_χ=0.51 based on a $1/S$

expansion. Although we are able to explain the one-magnon excitation spectrum, the $1/S$ expansion also predicts additional spectral weight [11] which has not yet been observed.

We now turn the metals $La_{1.86}Sr_{0.14}CuO_4$ and $YBa_2Cu_3O_{6.6}$. The response of the copper spins obeys the sum rule,

$$\left\langle m^2 \right\rangle = \frac{3\hbar}{\pi} \int_{-\infty}^{\infty} \frac{\chi''(\omega)\, d\omega}{1 - \exp(-\hbar\omega/kT)} \tag{10}$$

where $\langle m^2 \rangle$ is the mean squared moment on the Cu sites. In both superconductors studied here, doping and the consequential metal-insulator transition led to a large redistribution of spectral weight and formation of a peak in $\chi''(\omega)$ at intermediate frequency. In the light of the sum rule, the existence of the peak in itself is not unexpected since spectral weight is lost from the Bragg peak present in the insulator and the high frequency response is strongly suppressed. What is surprising is the relatively small energy scale over which the response is distributed compared with other paramagnetic metals. Such small electronic energy scales are, of course, characteristic of the cuprate superconductors.

REFERENCES

[1] See e.g. J. M. Tranquada, *et al.*, Phys. Rev. Lett. **60**, 156 (1988); J. Rossat-Mignot, *et al.*, Physica **185-189**, 86 (1991); H. A. Mook *et al.*, Phys. Rev. Lett. **70**, 3490 (1993); H. F. Fong *et al.*, Phys. Rev. Lett. **75**, 316 (1995).

[2] D. J. Scalapino, Phys. Rep. **250**, 329 (1995).

[3] G. Aeppli *et al.*, Phys. Rev. Lett. **62** 2052 (1989); S. M. Hayden *et al.*, Phys. Rev. Lett. **67**, 3622 (1991).

[4] S. M. Hayden *et al.*, Phys. Rev. Lett. **76**, 1344 (1996).

[5] S. M. Hayden *et al.*, Phys. Rev. B **54**, R6905 (1996).

[6] P. Dai *et al.*, unpublished.

[7] See, e.g. R. M. White, *Quantum Theory of Magnetism*, Springer Ser. Solid-State Sci., Vol. 32 (Springer, Berlin 1983) ch 8. Throughout this paper we use the reduced susceptibility as discussed in this reference.

[8] C. G. Windsor, *Pulsed Neutron Scattering* (Taylor and Francis, London, 1981).

[9] 0. Steinsvoll et al., Phys. Rev. B **30**, 2377 (1984).

[10] R. R. P. Singh, Phys. Rev. B **39**, 9760 (1989).

[11] J. Igarashi, Phys. Rev. B **46**, 10763 (1992); J. Phys.: Condens. Matter **4**, 10265 (1992).

[12] J. M. Tranquada, , Phys. Rev. B **40** 4503 (1989).

[13] D. Reznik *et al.*, Phys. Rev. B **53**, R14741. (1996).

[14] K. Yamada *et al.*, J. Phys. Soc. Jpn. **64**, 2742 (1995).

[15] P. Dai *et al.*, Phys. Rev. Lett. **77**, 5425 (1996).

[16] P. Dai *et al.*, cond-mat/9707112

[17] G. Aeppli *et al.*, unpublished.

FIGURES

FIG. 1. (a)-(f) Magnetic scattering from La_2CuO_4 and (g)-(l) from $La_{1.86}Sr_{0.14}CuO_4$ [4]. All scans are in the same absolute units. Note the magnetic peak is broader in the superconductor and suppressed at higher frequencies.

FIG. 2. Local susceptibility [4] derived from data such as that in Fig. 1 (closed circles) and from reactor-based measurements [17]. Note huge redistribution of spectral weight caused by doping.

FIG. 3. Constant energy scans showing magnetic scattering from $YBa_2Cu_3O_{6.15}$ for wavevectors $\mathbf{Q} = (h, h, l)$. (b)-(e) l chosen to emphasize acoustic modes. (g)-(j) l chosen to emphasize optic modes. The onset of scattering at the optic position is about 74 meV.

FIG. 4. Acoustic and optic contributions to the local or wavevector-integrated energy-dependent magnetic susceptibility in $YBa_2Cu_3O_{6.15}$. Points have been obtained by integrating over the spin-wave peaks and correcting for the Cu^{2+} magnetic form factor, Bose factor and instrumental resolution. Solid lines are a fit to the spin wave model described in the text.

FIG. 5. (a) Dispersion relation of $YBa_2Cu_3O_{6.15}$. Closed circles and solid line are acoustic mode. Open circles and dashed line are optic mode. (b)-(e) Constant energy scans showing the high-frequency magnetic scattering from $YBa_2Cu_3O_{6.15}$.

FIG. 6. Constant energy scans showing magnetic scattering from $YBa_2Cu_3O_{6.6}$ for wavevectors $\mathbf{Q} = (h, h, l)$. (a)-(c) l chosen to emphasize acoustic modes. (d)-(f) l chosen to emphasize optic modes.

FIG. 7. Acoustic and optic contributions to the local susceptibility in $YBa_2Cu_3O_{6.6}$. Solid lines are a guide to the eye.

TABLES

TABLE I. The table summarizes experimentally-determined spin-wave parameters for $La_{2-x}Sr_xCuO_4$ and $YBa_2Cu_3O_{6+x}$. In the case of the superconductors, $J_{||}^*$ and Z_c are determined from the highest frequencies studied.

	$J_{||}^*$	$J_{\perp}^*$	Z_χ	$\hbar\omega_g$
La_2CuO_4	153 meV		0.39 ± 0.1	
$La_{1.86}Sr_{0.14}CuO_4$	130 ± 5 meV		0.15 ± 0.06	
$YBa_2Cu_3O_{6.15}$	125 ± 5 meV	11 ± 2meV	0.4 ± 0.1	74 ± 5 meV
$YBa_2Cu_3O_{6.6}$				≈ 60 meV

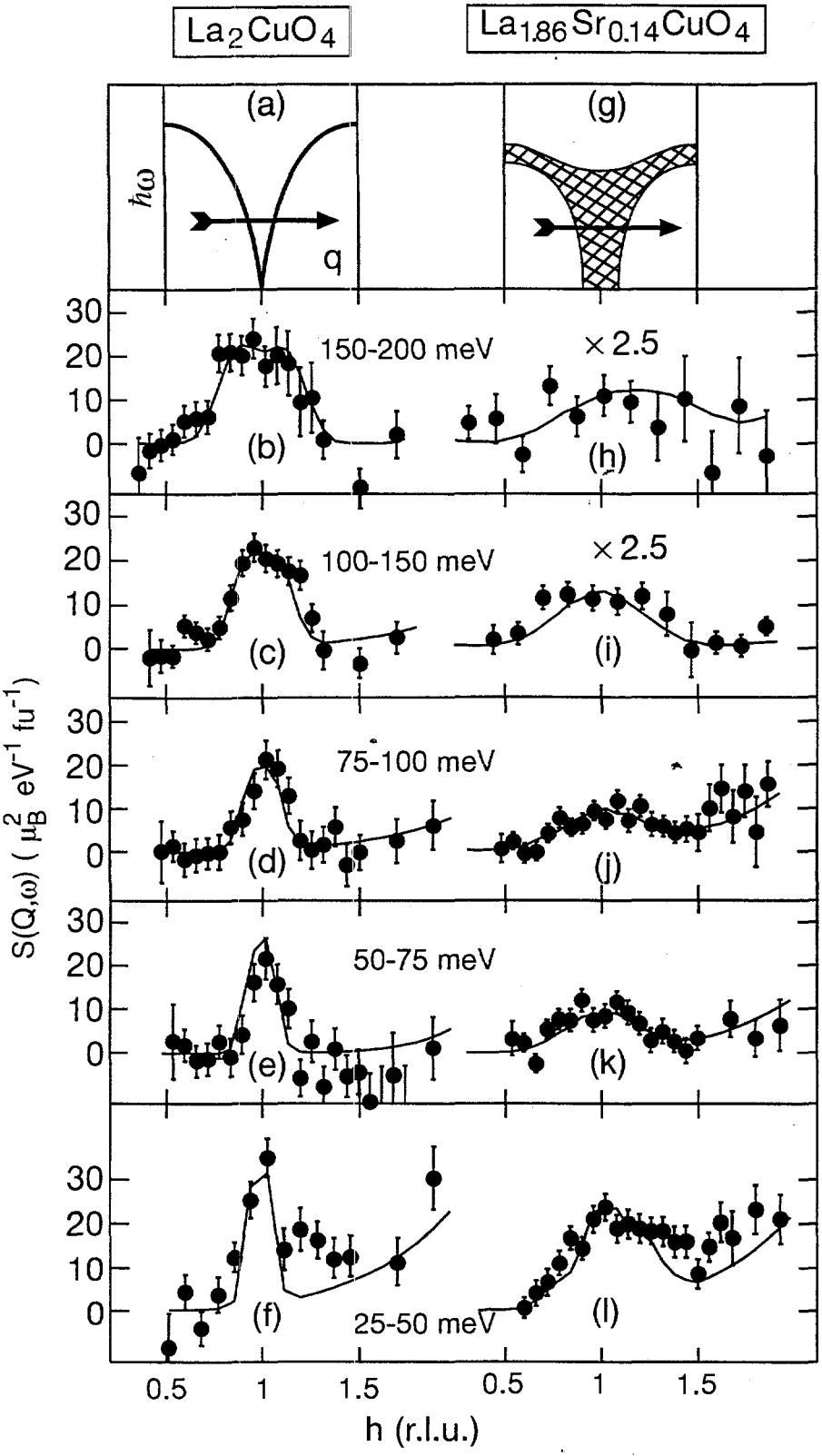

Hayden et al Fig. 1

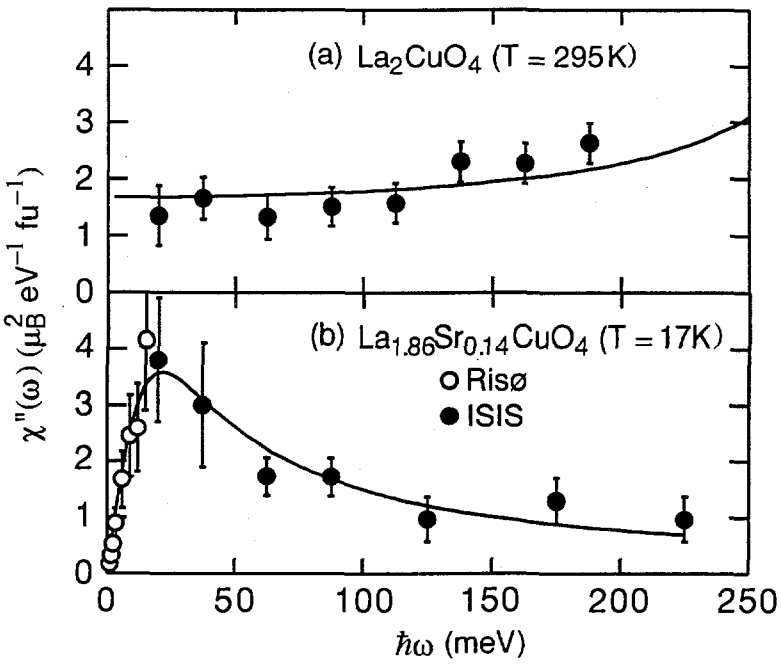

Hayden et al Fig. 2

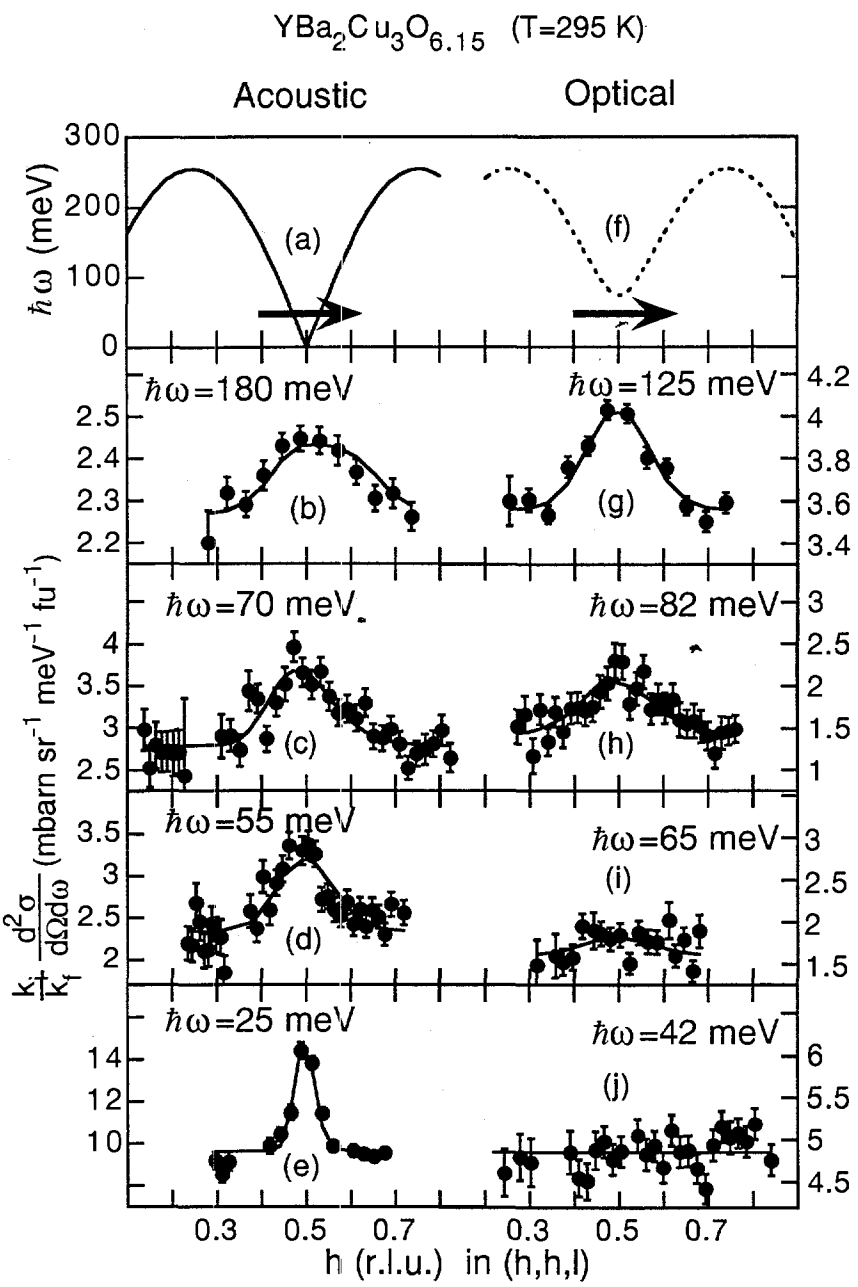

Hayden et al. Fig. 3

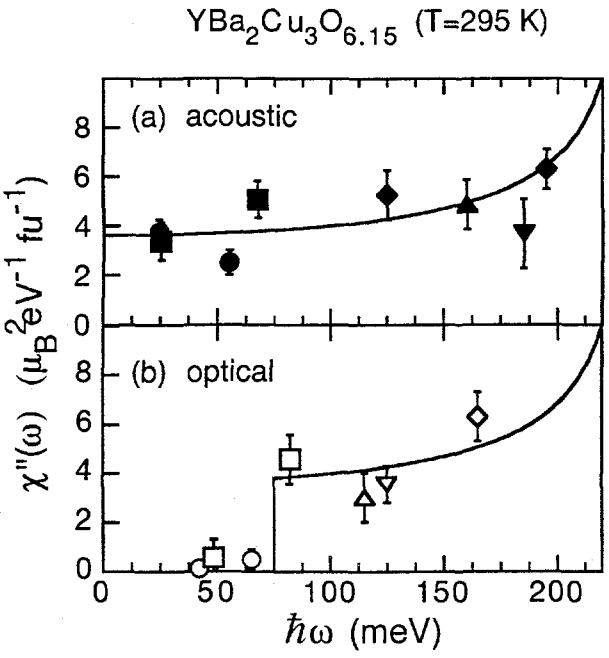

Hayden et al. Fig. 4

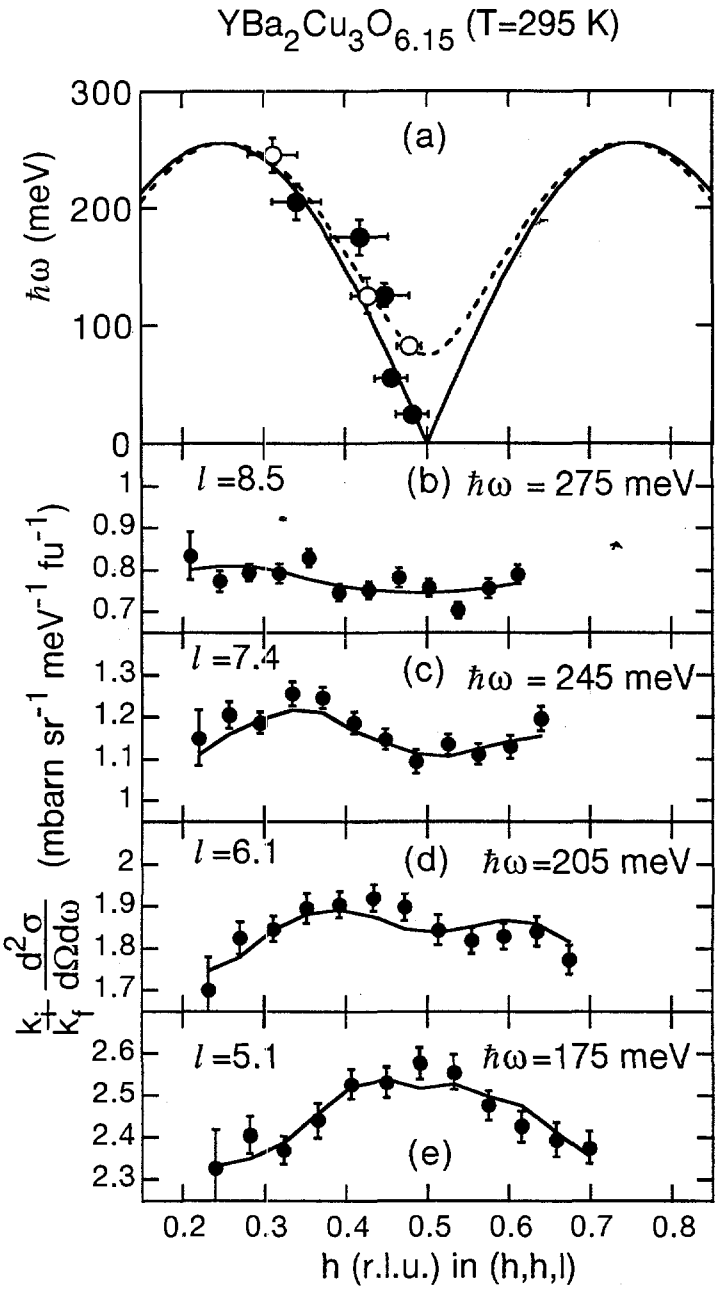

Hayden et al. Fig. 5

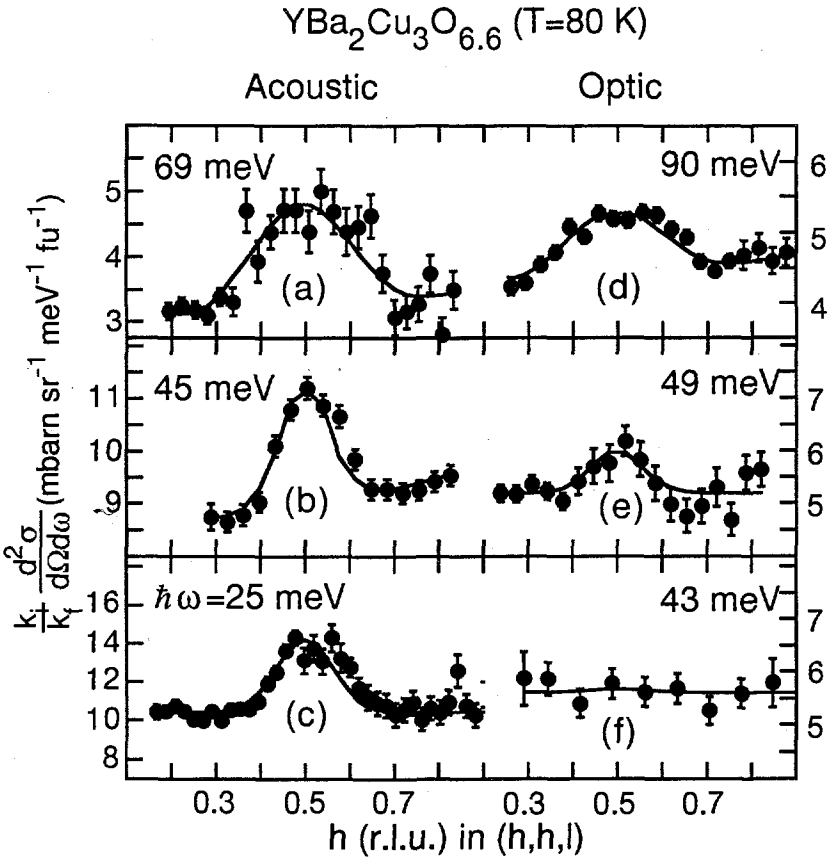

Hayden et al. Fig. 6

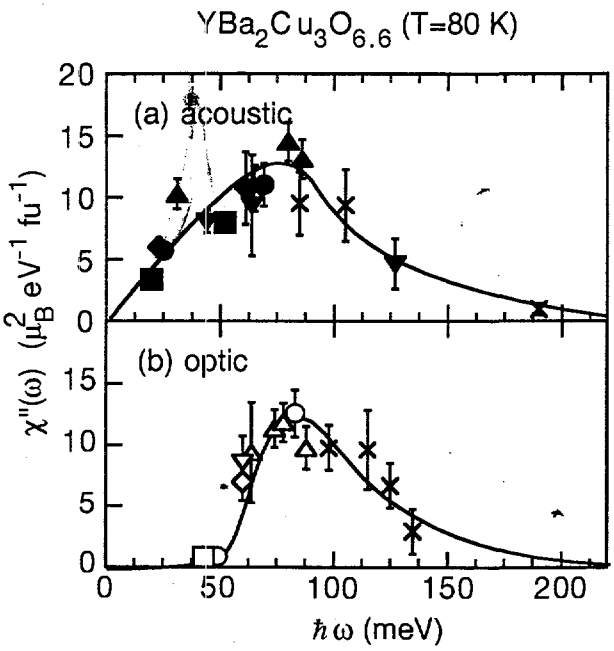

Hayden et al. Fig. 7